Quantifying Immune Checkpoint engagement in Patient Biopsies

Cristina Cacho-Navas[1], Laura Camacho[1], Jon Agüero[1], Baterdene Batmunkh[1], José María Gracia[1], Carlos Eduardo de Andrea[2], Salvador Martin Algarra[3], Markel Rementeria[1], James Miles[1], Juan Gumuzio[1], Fernando Aguirre[1], Peter J. Parker[4,5], Véronique Calleja[1].

[1] HAWK Biosystems (FASTBASE Solutions S.L.) 612 Astondo Bidea, Science and Technology Park of Bizkaia, Derio, Bizkaia, Spain.

[2] Facultad de Medicina, Departamento de Patología, Anatomía y Fisiología, Clínica Universidad de Navarra (CUN), Pamplona, Spain.

[3] Facultad de Medicina, Departamento de Oncología, Clínica Universidad de Navarra (CUN), Pamplona, Spain.

[4] School of Cancer and Pharmaceutical Sciences, King's College London, London, United Kingdom.

[5] Francis Crick Institute, London, United Kingdom.

Correspondence: Véronique Calleja (veronique.calleja@hawkbiosystems.com)

Keywords: Functional Proteomics, Spatial Biology, QF-Pro®, FRET-FLIM, Immuno-oncology, Precision Medicine

Abstract

Immune checkpoint blockade (ICB) has emerged as a transformative approach in cancer treatment showing remarkable results on previously untreatable cancers. Nevertheless, a high percentage of patients fail to respond to treatment and often suffer strong immune related adverse events (irAE). Therefore, it becomes critical to identify with high confidence the patients who will respond to ICB using robust predictive biomarkers. To date patient stratification to treatment using current FDA approved biomarkers like PD-L1 TPS score has been poor. Hence, we propose that biomarkers assessing immune checkpoint functional state should better reflect the actual immune status of the tumour microenvironment (TME). Here, we describe a methodology for assessing the interaction of a panel of immune checkpoints in tissue and tumour samples using a quantitative spatial proteomics approach (QF-Pro). The functional immune profiling of tumours has the potential to provide a more profound understanding of the mechanisms put in place by the tumour to evade immune surveillance and offers a unique opportunity for the development of personalised immunotherapy regimens.

Results and discussion

Immune checkpoints are essential regulatory pathways that maintain immune homeostasis and prevent excessive immune activation [1] (Fig.1A). In cancer, tumour cells evade immune surveillance by triggering immune checkpoint engagement [2, 3] and while immune checkpoint blockade (ICB) against PD-1/PD-L1 (nivolumab, pembrolizumab) or CTLA4 (ipilimumab), has shown remarkable benefits [4], a high percentage of patients fail to respond to treatment and often suffer strong immune related adverse events (irAE) [5, 6]. This is particularly visible in combination treatments like anti-PD-1 with anti-CTLA4 or the newly approved anti-LAG3 (relatlimab) in metastatic melanoma, where the improved response is accompanied by about 60% and 20% respectively of grade 3-4 side effects [7]. Therefore, it is critical to identify the patients who will respond to treatment. To do so, companion and complementary diagnostics are presently used. They encompass PD-L1 expression, tumour mutational burden (TMB) or T cell infiltration among others [8]. However, patient stratification to treatment using these biomarkers has been poor, highlighting the need for better predictive biomarkers. While new biomarkers are being investigated [9] none directly evaluate checkpoint engagement, the actual target of immune checkpoint blockade.

Biomarkers assessing immune checkpoint functional state would be expected to better reflect the actual immune status of the tumour microenvironment (TME). This was previously demonstrated for the well-studied PD-1/PD-L1 in NSCLC, where the stratification power associated with PD-1/PD-L1 engagement status in patient biopsies had shown far superior predictive value to current ICB treatment, compared to the routinely employed PD-L1 TPS score [10]. These results greatly encouraged the analysis

of a wider panel of immune checkpoints in tissue and tumour samples with the goal of evaluating their potential use in identifying new biomarkers and therapeutic opportunities in cancer.

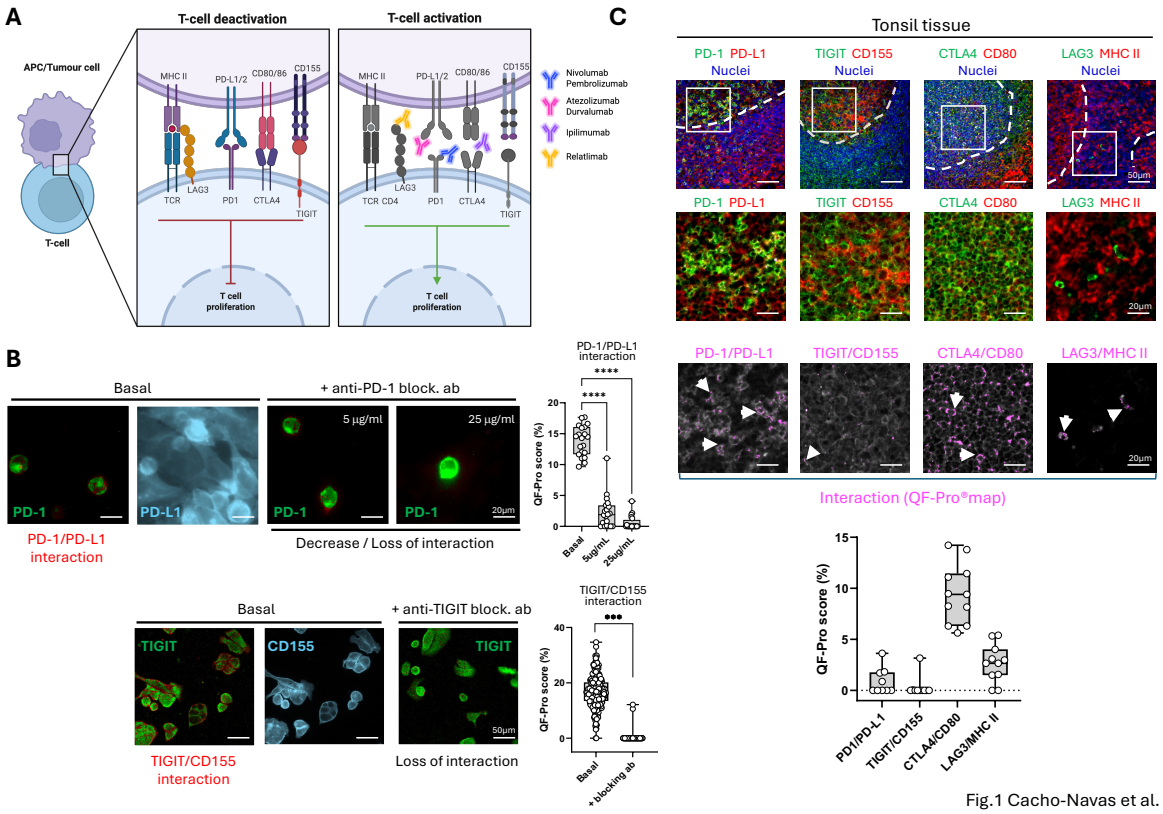

Figure 1: Quantitative measurement of immune checkpoint complex engagement in FFPE tissue samples. (A) Immune checkpoint complexes and their associated therapeutic monoclonal antibodies. **(B)** Validation of PD-1/PD-L1 and TIGIT/CD155 interaction in cells with blocking antibodies using Promega co-culture cell kits. Expression of the biomarkers are in green or blue as indicated and the interaction is shown in red and quantified in the box and whisker plots; P≤0.001(***); P≤0.0001(****). **(C)** Human FFPE tonsil was labelled to quantify immune checkpoint interactions. The expression of the donor (green), acceptor (red) and nuclei (blue). The interaction localisation (QF-Pro® map) of immune checkpoint engagement is shown in magenta overlayed with the donor expression (grey). The box and whisker plot shows the quantitative interaction scores for each biomarker. Dots correspond to fields of interest.

QF-Pro® (Quantifying Functions in Proteins) is an enhanced FRET/FLIM-based imaging technology developed to measure the functional states of proteins in fixed cells or tissue samples (FFPE) (Supplementary Fig. 1 and Materials & Methods). This method enables

46 the quantification of both intracellular and intercellular protein-protein interactions as
47 well as bringing specificity to the monitoring of post-translational modifications in
48 complex biological microenvironments. The technology uses advanced amplified
49 immunolabeling and imaging to spatially quantify functional states *in-situ*, requiring
50 careful selection and characterisation of reagents as a prelude to their application.

51 To determine the specificity of the reagents selected (primary and QF-Pro® secondary
52 Abs), in-cell assays were performed. Figure 1B shows an example of the validation of the
53 reagents for PD1/PDL1 and TIGIT/CD155 checkpoints measurement signal in CHO-
54 K1/Jurkat cells co-cultures treated or not with a blocking antibody against PD-1 or TIGIT
55 respectively before fixation. The loss of interaction signals following blockade with
56 specific interfering antibodies are presented in box-and-whisker plots demonstrating the
57 specificity of the immune complex engagement signals afforded by these reagents.

58 To determine whether these and other validated pairings would translate to tissue
59 sections, human FFPE-tonsil tissue was chosen as a proof-of-concept model. This
60 lymphoid organ plays a crucial role in early immune priming and response where multiple
61 immune cells interact with antigen presenting cells [11]. Hence the level of interaction of
62 four identified and promising immune checkpoints (PD-1/PD-L1, CTLA4/CD80,
63 TIGIT/CD155 and LAG3/MHC II) [12] was quantified. The interaction quantification (QF-
64 Pro® scores) and localisation (QF-Pro® maps) for all the checkpoints was determined in
65 addition to the expression of the immune receptors and their ligands (green and red) in
66 the DAPI stained tissue (Fig. 1C). The data reflected the variability in interaction scores
67 and specific localisation of the different checkpoints in the same tissue.

The success of these immune checkpoint quantifications in tonsil tissue encouraged the analysis of these interactions in various tumour tissues. The determination of a functional immune signature, directly within FFPE tumour samples, could in principle be used to aid patient stratification to ICI therapies in tumours. To assess the robustness of the method various types of tumour samples with different histological characteristics were analysed. In Figure 2A, the localisation of PD-1/PD-L1 interaction is observed within both NSCLC and melanoma biopsies. The interaction scores (in %) quantify the interaction states between tumour cells and infiltrating immune cells visible in pink in the interaction maps.

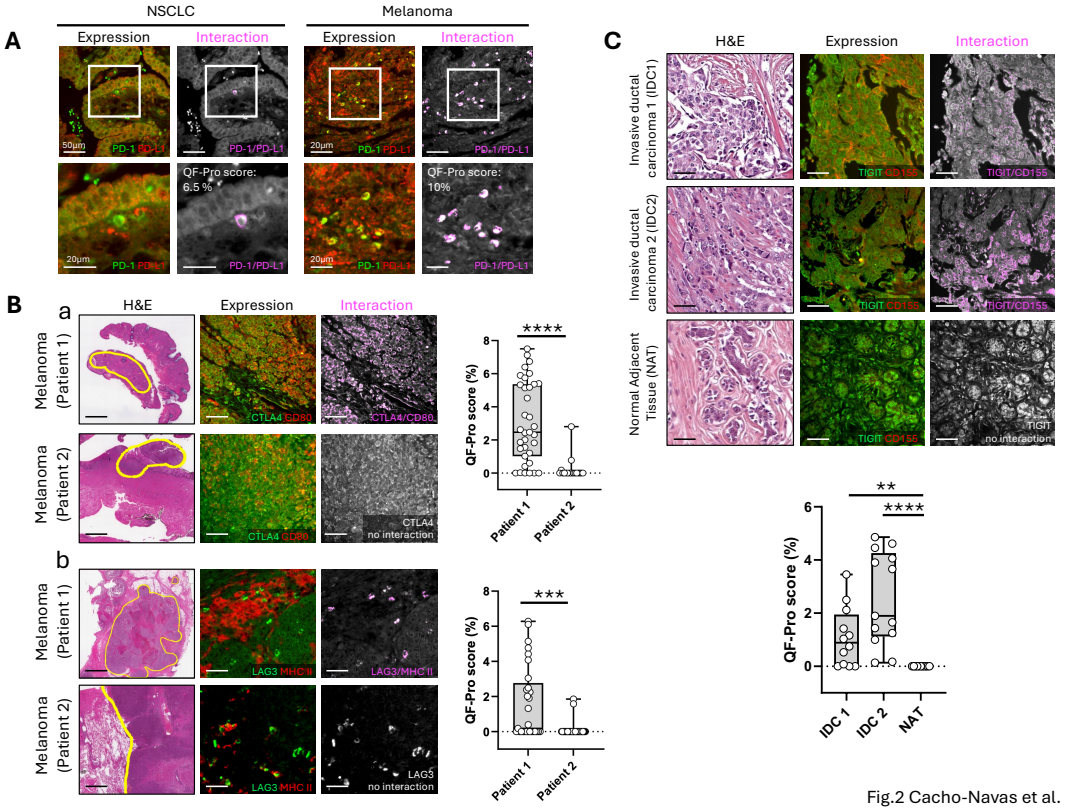

Figure 2: Spatial quantification and profiling of immune checkpoint engagement by QF-Pro® in tumours. Within all images, immune checkpoint receptors are green, ligands red and the complex engagement localisation in magenta. **(A)** PD-1/PD-L1 expression and engagement (in %) overlayed in NSCLC and melanoma. **(B)** H&E staining of 4 patients' melanoma biopsies showing tumoral areas (yellow). CTLA4/CD80 and LAG3/MHC II expression and interaction in melanoma. Box-and-whisker plots show the different engagement in these patients. Each dot corresponds to one field of interest. **(C)** H&E, TIGIT/CD155 expression and interaction in a TMA with invasive ductal carcinomas (IDCs) and normal adjacent tissue

(NAT) of the breast. In all experiments P≤0.01(**), P≤0.001(***) and P≤0.0001(****). The scale bars on the fluorescence images in B and C represent 50µm. Scale bar on the H&E is 4mm (B) and 50µm (C).

In advance metastatic melanoma both anti-CTLA4 and anti-LAG3 therapies in combination with anti-PD-1 have been used, therefore we assessed whether a direct quantification of CTLA4/CD80 (Fig.2 B panel a) and LAG3/MHC II (Fig.2 B panel b) engagement could be performed in patient's biopsies. The primary melanoma tumour regions were identified by a pathologist (H&E, yellow). The images show the expression of immune receptors CTLA4 and LAG3 (green) and respective ligands CD80 and MHC II (red) and the interaction maps in magenta. Quantification of CTLA4/CD80 interaction demonstrated a significant difference in interaction states between two patients' skin tumour despite a similar colocalization of the proteins (green and red labelling) in both samples (Fig.2 B panel a). Similarly, the level of LAG3/MHC II interaction measured in the two patients showed very different interaction scores, despite the similar level of expression of the two proteins (Fig.2 B panel b). These results clearly illustrate the need for measuring the level of engagement to inform on the potential value of intervention. The sole expression of the checkpoint proteins used as a surrogate for the interaction can clearly be inadequate as shown in this example.

In invasive breast cancer (invasive ductal carcinoma - IDC) the upregulation of TIGIT expression has been associated with bad prognosis, suggesting TIGIT/CD155 involvement in the negative regulation of immune response in the TME [13]. These observations imply that this checkpoint could potentially be a good target to immune checkpoint blockade providing the presence of a suitable biomarker. In Figure 2C, TIGIT/CD155 interaction was identified in a TMA containing two different IDCs and one

normal adjacent tissue (NAT). The quantification of TIGIT/CD155 expression shows the variability of the interaction in two IDC patients and as predicted a lack of interaction in the non tumoural tissue. Evidently, this complex can be assessed and indeed can be engaged in IDC suggesting that it should be assessed in the context of intended immune checkpoint blocade.

The analysis of immune checkpoints has become paramount in the correct diagnosis and treament of a range of tumours. Until now, the expression levels of immune checkpoint receptors or ligands have been used as gold standards for predicting response rates to immune checkpoints inhibitors. However, the inability to reliably identify responders vs non-responders has encouraged the discovery of new biomarkers. The excellent predictive value of PD-1/PD-L1 engagement shown in NSCLC [10] highlights the importance of exploiting functional biomarkers to predict patient response to ICIs. Here, we demonstrate that by using QF-Pro® we can identify and spatially quantify the interaction of a variety of immune checkpoints in different tissues.

The primary involvement of multiple checkpoints in parallel, alongside adaptive resistance to checkpoint blockade, has led to the need for the simultaneous analysis of multiple checkpoints to inform on the most appropriate treatment option(s). The functional immune profiling of tumours has the potential to provide a deeper and more accurate understanding of the mechanisms put in place by the tumour to evade immune surveillance and offers a unique opportunity for the development of personalised immunotherapy regimens.

121 ## Materials and methods

122 **Primary antibodies**

Antibody	Catalogue Number
Recombinant anti-PD-1 NAT105 mouse mAb	ab234444
Anti-PD-L1 28-8 rabbit mAb	ab205921
Anti-TIGIT 4A10 mouse mAb	RF16054
Anti-CD155 rabbit mAb	NBP2-78711
Anti-LAG3 mouse mAb	ab307517
Anti-MHC II rabbit mAb	ab92511
Anti-CTLA4 mouse mAb	ABIN6992223
Anti-CD80 rabbit polyclonal Ab	MBS2522916
Blocking TIGIT antibody	Promega J2051
Blocking PD-1 antibody	Promega J1201

123

124 **Secondary reagents**

125 QF-Pro® reagent kits contain all reagents needed to perform the labelling process. Briefly,
126 the reagents provided within the kit include peroxidase suppressor, blocking and washing
127 buffers, fluorescent (ATTO488 and AlexaFluor594) labelled secondary anti-mouse and
128 anti-rabbit antibodies, amplification reagents and mounting medium.

129 **FFPE- tissue and tumour samples**

130 Formalin-fixed, paraffin-embedded (FFPE) sections of 3-5 μm thickness were obtained
131 from diagnostic biopsies, tumour resections or healthy tissues. Melanoma samples were
132 provided by the Pathology Department of Clínica Universidad de Navarra (CUN). Tonsil
133 blocks and TMA slides of breast tumours were purchased from Amsbio. FFPE samples
134 were stained with H&E following standard protocol.

135 **QF-Pro® (Quantifying Function in Proteins) Assay**

136 Before incubation with QF-Pro® reagents, pre-treatment processes of deparaffination,
137 rehydration and epitope retrieval were performed using a Dako PT-Link. Samples were
138 then treated following the QF-Pro® labelling protocol. Briefly, samples were incubated
139 with endogenous peroxidase suppressor and then with blocking buffer to prevent non-
140 specific signal. Samples were incubated with primary antibodies overnight at 4°C and
141 then with donor and acceptor secondary reagents at room temperature (RT) for two
142 hours. Amplification reagent was applied to Donor-Acceptor slides for 20 minutes and
143 mounting medium was applied. Slides were stored until ready for fluorescence lifetime
144 imaging microscopy analysis. A detailed protocol for QF-Pro® assays can be found in our
145 previous publications [10, 14].

146 **Acquisition, analysis and quantification**

147 Imaging and quantification of the immune checkpoint interaction states were performed
148 using Violet 3.0. (Fluorescence Lifetime Imaging Microscope), controlled by QF-Pro®
149 software. Violet 3.0 and QF-Pro® software automatically measure the decay of the
150 lifetime of the donor fluorophore in the absence and presence of the acceptor (FRET-
151 FLIM) to calculate interaction states (QF-Pro® scores). Violet 3.0 and QF-Pro® software
152 allow for the spatial quantification of proteomic functional events across the sample.

153 **Cell cultures and sensitivity assays**

154 The commercially validated Promega Blockade Bioassay kits, originally designed to
155 measure the antibody blockade of PD-1/PD-L1 and TIGIT/CD155 interaction by
156 luminescence, were adapted for performing QF-Pro® protocol. Cells were thawed and
157 directly used in this assay following the recommendations of the manufacturer. PD-L1 or
158 CD155–expressing CHO-K1 cells were seeded onto 96 well plates and were incubated at

159 37 °C with 5% CO_2 for 16 hours. PD-1 or TIGIT–expressing Jurkat cells together with the

160 blocking antibodies (against PD-1 or TIGIT respectively) were added to the CHO-K1cells.

161 The co-cultures were incubated for 20 hours at 37°C with 5% CO_2. The unbound cells

162 were removed by washing with PBS before being fixed with 4% PFA for 15 minutes. After

163 fixation, cells were washed with PBS and stored at 4 ºC until labelling. QF-Pro® labelling

164 was performed as described for FFPE-samples.

Authors contribution

All authors listed have made a substantial contribution to the work and approved it for publication. C.C.N and L.C. designed and performed the QF-Pro® experiments on FFPE samples. J.G., M.R. and J.M. designed and performed QF-Pro® experiments on cells assays. C.E.A and S.M.A carried out patient recruitment and provided FFPE tumour samples. J.A., B.B., J.M. and F.A. were involved in the development of the QF-Pro® FLIM platform. C.C.N, L.C. and V.C. were involved in the writing of the manuscript. P.J.P, J.G. and J.M. were involved in the critical reading of the manuscript. All authors read and approved the final manuscript.

Acknowledgments

This work was supported in part by the PREDICTIM project grant number CPP2021-008390. We would like to thank Elena Castellano Sanz for assisting with the figures illustrations.

Conflict of interest

C.C.N, L.C, J.A, B.B, J.M.G, J.M, J.G, M.R, F.A, V.C. are employees of HAWK Biosystems which hold the patent to the iFRET technology employed in this paper. P.J.P retains financial interest in HAWK.

Ethics statement

The melanoma samples use are part of a study that was approved by the ethics committee of the University of Navarra, Spain (protocol 111/2010). FFPE tissue samples were obtained with informed patients' consent and retrieved from the pathology files of the Clínica Universidad de Navarra.

Data availability statement

The data that support the findings of this study are available from the corresponding author upon reasonable request.

References

1. Abdeladhim, M., J.L. Karnell, and S.A. Rieder, *In or out of control: Modulating regulatory T cell homeostasis and function with immune checkpoint pathways.* Front Immunol, 2022. **13**: p. 1033705.
2. Galassi, C., et al., *The hallmarks of cancer immune evasion.* Cancer Cell, 2024. **42**(11): p. 1825-1863.
3. He, X. and C. Xu, *Immune checkpoint signaling and cancer immunotherapy.* Cell Res, 2020. **30**(8): p. 660-669.
4. Kong, X., et al., *Immune checkpoint inhibitors: breakthroughs in cancer treatment.* Cancer Biol Med, 2024. **21**(6): p. 451-72.
5. Berland, L., et al., *Further knowledge and developments in resistance mechanisms to immune checkpoint inhibitors.* Front Immunol, 2024. **15**: p. 1384121.
6. Iranzo, P., et al., *Overview of Checkpoint Inhibitors Mechanism of Action: Role of Immune-Related Adverse Events and Their Treatment on Progression of Underlying Cancer.* Front Med (Lausanne), 2022. **9**: p. 875974.
7. Kreft, S. and P. Lorigan, *Combination Immunotherapy for Advanced Melanoma-How to Choose?* J Clin Oncol, 2025. **43**(4): p. 478-479.
8. Twomey, J.D. and B. Zhang, *Cancer Immunotherapy Update: FDA-Approved Checkpoint Inhibitors and Companion Diagnostics.* AAPS J, 2021. **23**(2): p. 39.
9. Yamaguchi, H., et al., *Advances and prospects of biomarkers for immune checkpoint inhibitors.* Cell Rep Med, 2024. **5**(7): p. 101621.
10. Sanchez-Magraner, L., et al., *Functional Engagement of the PD-1/PD-L1 Complex But Not PD-L1 Expression Is Highly Predictive of Patient Response to Immunotherapy in Non-Small-Cell Lung Cancer.* J Clin Oncol, 2023. **41**(14): p. 2561-2570.
11. Massoni-Badosa, R., et al., *An atlas of cells in the human tonsil.* Immunity, 2024. **57**(2): p. 379-399 e18.
12. Lu, C. and Y. Tan, *Promising immunotherapy targets: TIM3, LAG3, and TIGIT joined the party.* Mol Ther Oncol, 2024. **32**(1): p. 200773.
13. Guo, C., et al., *TIGIT as a Novel Prognostic Marker for Immune Infiltration in Invasive Breast Cancer.* Comb Chem High Throughput Screen, 2023. **26**(3): p. 639-651.
14. Sanchez-Magraner, L., et al., *High PD-1/PD-L1 Checkpoint Interaction Infers Tumor Selection and Therapeutic Sensitivity to Anti-PD-1/PD-L1 Treatment.* Cancer Res, 2020. **80**(19): p. 4244-4257.